

WIENER PREDICTION-BASED CHANGE DETECTION FOR LOCATING MINES IN MULTILOOK SAR IMAGERY

Nasser M. Nasrabadi

U.S. Army Research Laboratory, 2800 Powder Mill Rd., Adelphi, MD 20783

1. INTRODUCTION

In this paper, we present a Wiener-based change detection method and compare its performance with several other methods for a pair of multi-look synthetic aperture radar (SAR) images of the same scene. Among the simple methods that are implemented for comparison are differencing, Euclidean distance, and image ratioing [1]. These methods require minimal processing time, with little computational complexity, and incorporate no statistical information. We also implemented methods which incorporate second order statistic calculations in making a change decision in efforts to mitigate false alarms arising from the speckle noise, misregistration errors, and nonlinear variations in SAR images. These methods include the proposed Wiener prediction-based method, Mahalanobis distance measure and subspace projection methods [2]. We compare the performance of these methods using multi-look SAR images containing several targets (mines). We present results in the form of receiver operating characteristics (ROC) curves.

2. EUCLIDEAN DISTANCE, IMAGE RATIOING CHANGE DETECTION METHODS

In simple difference-based change detection a pixel from one image (the reference image) is subtracted from the pixel in the corresponding location of another image (the test image) which has changed with respect to the reference image. One can also subtract a block of pixels from one image from the corresponding block from a test image. This is referred to as Euclidean difference if the blocks of pixels are arranged into vectors and the L-2 norm of the difference of these vectors is computed. We implemented the Euclidean distance as in (1) where we computed the L-2 norm of the difference between a block of pixels (arranged into a 1 dimensional vector) from reference image, \mathbf{f}_X , and the corresponding block in the test image, \mathbf{f}_Y , to obtain an error, $e_E(i, j) = \|\mathbf{y}_{ij} - \mathbf{x}_{ij}\|$ where \mathbf{x} and \mathbf{y} are vectors of pixels taken from \mathbf{f}_X and \mathbf{f}_Y , respectively at location (i, j) . When no change has occurred, this error is expected to be low and the error will be high when a change has occurred. Closely related to the Euclidean distance metric for change detection is image ratioing. It is implemented as

$e_R(i, j) = \frac{y_{ij}}{x_{ij}}$ where y_{ij} and x_{ij} are pixels from the same locations in the test and reference images, respectively.

3. MAHALANOBIS DISTANCE, SUBSPACE PROJECTION-BASED AND WIENER PRECICTION-BASED CHANGE DETECTION

In Mahalanobis distance-based change detection, we obtain an error (change) image by computing the Mahalanobis distance between \mathbf{x} and \mathbf{y} to obtain $e_{MD}(i, j) = \sqrt{(\mathbf{x}_{ij} - \mathbf{y}_{ij})^T \mathbf{C}_X^{-1} (\mathbf{x}_{ij} - \mathbf{y}_{ij})}$. The \mathbf{C}_X^{-1} term in the Mahalanobis distance is the inverse covariance matrix computed from vectors of pixels in \mathbf{f}_X . By considering the effects of other pixels in making a change decision with the inclusion of second order statistics, the Mahalanobis distance method is expected to reduce the false alarms. In the case of subspace projection for change detection a subspace must be defined for either the reference or test image. We compute the covariance of a sample from \mathbf{f}_X and its eigenvectors \mathbf{V} and eigenvalues $\mathbf{\Lambda}$ as $\mathbf{C}_X = \mathbf{V}\mathbf{\Lambda}\mathbf{V}^T$. We truncate the number of eigenvectors in \mathbf{V} , denoted by $\tilde{\mathbf{V}}$, to develop a subspace projection operator $\mathbf{P}_X = \tilde{\mathbf{V}}\tilde{\mathbf{V}}^T$. The projection of the test image onto the subspace of the reference image will provide a measure of how much of the test sample is represented by the reference image. Therefore, by computing the squared difference between the test image and its projection onto the subspace

of the reference image we obtain an estimate of the difference between the two images, $e_{SP}(i, j) = \sqrt{[\mathbf{y}_{ij}^T (\mathbf{I} - \mathbf{P}_X) \mathbf{y}_{ij}]}$. In our implementations we include the \mathbf{C}_X^{-1} term in the subspace projection error term as $e'_{SP}(i, j) = \sqrt{[\mathbf{y}_{ij}^T (\mathbf{I} - \mathbf{P}_X)^T \mathbf{C}_X^{-1} (\mathbf{I} - \mathbf{P}_X) \mathbf{y}_{ij}]}$. The Wiener filter [3] is the linear minimum mean-squared error estimator for second-order stationary data. Consider the signal $\hat{\mathbf{y}}_{ij} = \mathbf{W} \mathbf{x}_{ij}$. The goal of Wiener filtering is to find \mathbf{W} which minimizes the error, $e_W(i, j) = \|\mathbf{y}_{ij} - \hat{\mathbf{y}}_{ij}\|$, where \mathbf{y} represents a desired signal. In the case of change detection \mathbf{y} is taken from the test image, \mathbf{f}_Y , which contains changes as compared to the reference image, \mathbf{f}_X . The Wiener filter seeks the value of \mathbf{W} which minimizes the mean squared error, which it found to be $\mathbf{W} = \mathbf{R}_{YX} \mathbf{R}_{XX}^{-1}$ where \mathbf{R}_{YX} is the cross correlation matrix of \mathbf{X} and \mathbf{Y} , and \mathbf{R}_{XX}^{-1} is the auto correlation matrix of \mathbf{X} . In a modified implementation of the Wiener prediction-based change detection method, we insert a normalization (or whitening) term, \mathbf{C}_X^{-1} , into the error equation as follows $e'_W(i, j) = \sqrt{(\mathbf{y}_{ij} - \hat{\mathbf{y}}_{ij})^T \mathbf{C}_X^{-1} (\mathbf{y}_{ij} - \hat{\mathbf{y}}_{ij})}$.

4. EXPERIMENTAL RESULTS

Results from all the methods implemented in this paper were normalized between zero and one before producing ROC curves. We used multi-look data collected at X band from a high resolution, VV-polarized SAR system (Fig. 1a and 1b). Small mines, comprising about a 5x5 pixel area, appear in the test image (Fig. 1b). The size of both the reference and test image is 950x950 pixels. Ground truth was provided which indicates the approximate center location of the known mines; we defined the mine area as an area slightly bigger than the average mine, centered at the locations indicated by ground truth information. To determine the performance, a hit was tabulated if at least a single pixel within the mine area surpassed the threshold. Any pixel outside of a mine area which surpassed the threshold was counted as a false alarm. A plot of the ROC curves for all the methods implemented is displayed in Fig. 2 for comparison. Local Wiener with \mathbf{C}_X^{-1} , local Mahalanobis, local subspace projection with \mathbf{C}_X^{-1} , and ratio methods all show similar performance. However, the local Mahalanobis distance method begins to perform worst than the others from about .4 to .65 probability of detection (Pd) rate, then surpasses all the other methods above Pd = .65. The simple difference method has the worst performance over all probability detection rates.

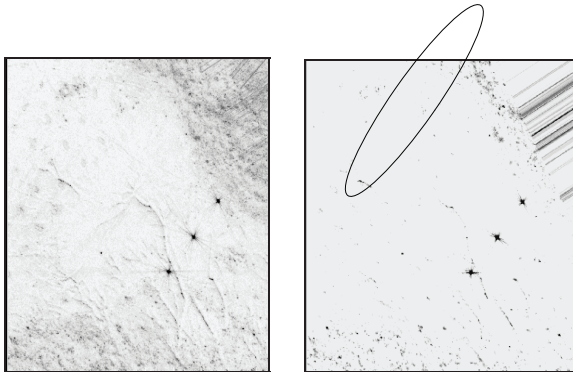


Fig.1 Original SAR Images: (a) Reference image, (b) Test image with mines contained in elliptical area.

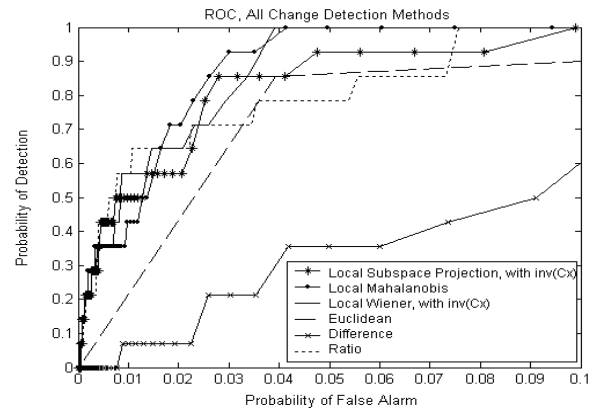


Fig. 2 ROC curves displaying performance of the various change detection methods implemented in this paper.

5. REFERENCES

- [1] J. F. Mas, "Monitoring land-cover changes: a comparison of change detection techniques," *International Journal of Remote Sensing*, vol. 20, no. 1, pp. 139-152, 1999.
- [2] H. Kwon, S. Z. Der and N. M. Nasrabadi, "Projection-based adaptive anomaly detection for hyperspectral imagery," *Proc. of IEEE International Conference on Image Processing*, pp. 1001-1004, 2003.
- [3] L. Scharf, *Statistical Signal Processing: Detection Estimation, and Time Series Analysis*, Addison Wesley, Colorado, 1991.